

# First Demonstration of a Single- $\lambda$ , Full-Duplex RRH Transceiver with Single RF Carrier for Bidirectional Radio

Bernhard Schrenk<sup>(1)</sup>, and Fotini Karinou<sup>(2)</sup>

<sup>(1)</sup>AIT Austrian Institute of Technology, Center for Digital Safety&Security / Security & Communication Technologies, 1210 Vienna, Austria.

Author e-mail address: bernhard.schrenk@ait.ac.at

<sup>(2)</sup>Microsoft Research Ltd., 21 Station Road, Cambridge CB1 2FB, United Kingdom.

**Abstract:** We successfully the reception and transmission of radio signals over the same opto-electronic port and at the same RF carrier frequency at the same time. We find  $>2\%$  EVM margins for 16/64-QAM OFDM down-/uplink transmission.

## 1. Introduction

The network densification inherent to the roll-out of 5G radio access enforces a widespread deployment of a large number of remote radio heads (RRH). Given the premise for cost efficiency, a functional split towards analogue radio-over-fiber transmission is preferable [1] as it greatly simplifies the field-installed RRH equipment. Such has been demonstrated by earlier works, aiming at radio channel aggregation, and now striving towards mm-wave bands [2,3]. The optical layer can be further simplified by facilitating full-duplex transmission over a single transceiver component that is shared between down- and uplink. Towards this direction, dual-function modulator/detector elements such as the electro-absorption modulator (EAM) [4,5] have been investigated in the past [6-8]. However, up to now there has been no work that facilitates down- and uplink transmission over the same wavelength and the same RF carrier frequency at the same time. This is because the power levels of the received optical downlink signal and the simultaneously transmitted RF uplink signal greatly differ at the common opto-electronic interface: the uplink is launched at a  $\sim 7$  orders-of-magnitude stronger level than the detected downlink is received. This renders techniques for crosstalk mitigation as indispensable. In earlier works, in-band crosstalk is avoided through the adoption of a paired signal spectrum in combination with frequency division duplexing (FDD) and frequency up/down conversion [6,7]. Alternatively, time division duplexing (TDD) can be adopted at the optical layer [8], but requires fast signal switching synchronized to the RF layer.

In this work, we experimentally demonstrate, for the first time to our best knowledge, full-duplex transmission of radio signals, utilizing a single-port transceiver operating a shared RF carrier for down- and uplink radio with overlapping signal spectra in the optical and RF domain. As such, the optical layer becomes fully transparent to the radio signal, thus contributing to the simplification of RRHs. We will prove the efficiency of the single- $\lambda/f_{RF}$  concept through crosstalk mitigation that enables a  $>2\%$  EVM margin for 16/64-QAM OFDM down/uplink transmission.

## 2. Single-Carrier Radio Communication over Single-Port, Dual-Function Optical Transceiver

Figure 1 presents the methodology. Full-duplex transmission over a single RF interface for modulation and detection requires a dual-function transceiver. Towards this, we expand our recent work on an electro-absorption modulated laser (EML) transceiver [9]. Coherent detection is achieved by beating its DFB emission with the received downlink. Since the DFB is subject to optical injection by the downlink, homodyne detection is accomplished. The EAM further takes a roll as dual-function photodiode/modulator element and is simultaneously re-used as uplink transmitter. A detailed treatment can be found in [9].

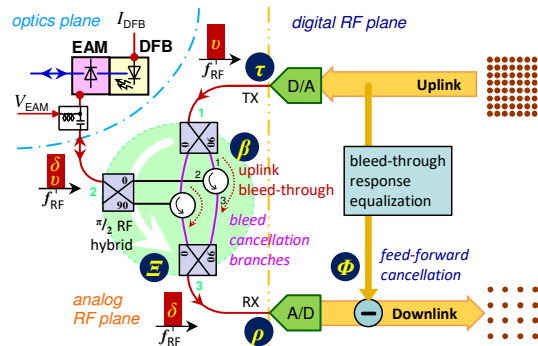


Fig. 1. RRH transceiver for full-duplex down/uplink transmission.

The overlapping spectra for down- and uplink require a good separation between these signals with a “colorless” directional splitter, especially due to the high dynamic range in RF power. A straightforward solution would be the use of a RF circulator at the EAM port. However, unlike optical circulators, there is strong bleed-through between ports 1 and 3 of a (multi-junction) RF circulator ( $\beta$ ). Figure 2a reports the native isolation ( $\nu$ ) between these ports of two RF circulators as later incorporated in the experiment. The native isolation is rather low over its operating bandwidth from 4 to 8 GHz. It shows a maximum of only 43.9 dB due to a resonance ( $\circ$ ). For this reason of insufficient uplink crosstalk suppression, we modified the circulating stage by incorporating a bleed-cancelling circuit. The circulating stage  $\mathcal{E}$  is split in two branches, which are constructively combined from the RF transmit port  $\tau$  to the EAM and also from the EAM to the receiver, while the bleed-through through the circulators is destructively combined towards the reception port  $\rho$ . As it is reported in Fig. 2a for two different implementations, the isolation ( $\blacklozenge, \blacksquare$ ) is improved over the entire spectrum and shows a new maximum that is improved by more than 15 dB ( $\blacksquare$ ). The ripple in the response and the limited bandwidth of the isolation maxima ( $\xi$ ) of  $\sim 120$  MHz ( $\blacklozenge$ ) is explained by the limited ability to precisely balance both cancellation branches in phase and, more importantly, loss over a broadband range when using discrete RF components. Here, we chose to optimize the balance for a high RF carrier frequency in the sub-6GHz range. The insertion loss between the EAM and RF receiver ( $\rho$ ) ports was 1.5 dB ( $\blacktriangle$ ) at 5.4 GHz. A similar value applies between the RF transmitter ( $\tau$ ) and EAM ports.

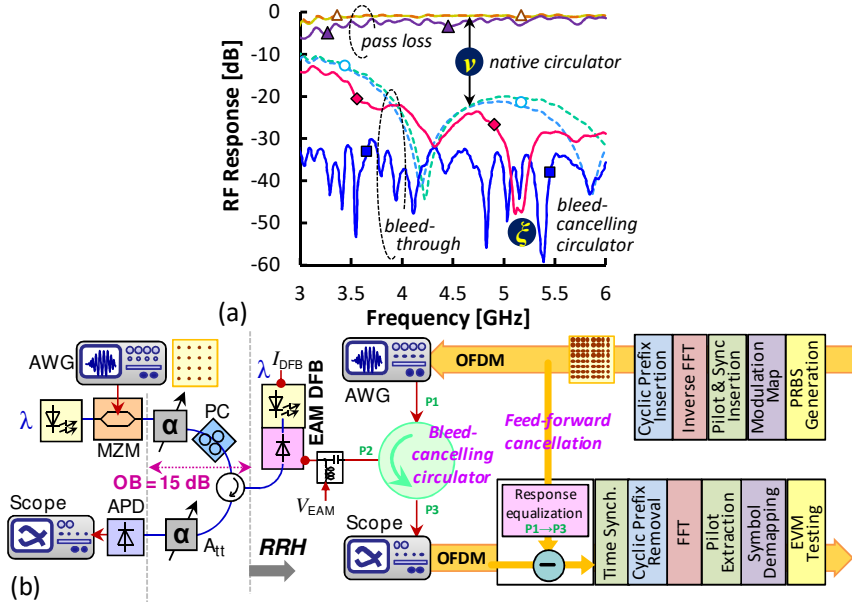


Fig. 2. (a) Response of standard and bleed-cancelling RF circulator for full-duplex RRH interface. (b) Experimental setup.

The achieved isolation of up to 59 dB, which foremost contributes to the crosstalk suppression of uplink bleed-through to the reception port ( $\rho$ ), also guarantees that the compound received signal, even though it still contains crosstalk noise, now adheres to the dynamic range of ADC without a much stronger uplink bleed-through determining the ADC scaling. This means that in-band uplink noise can be further mitigated by a simple digital feed-forward cancellation ( $\Phi$ ). Such a cancellation circuit, which involves channel sounding over the analogue RF circulation stage  $\mathcal{E}$  between DAC and ADC, has been additionally used in order to boost the SNR.

### 3. Experimental Setup

The proposed RRH transceiver has been evaluated in the experimental setup shown in Fig. 2b. The downlink OFDM at a RF carrier frequency of  $f_{RF} = 5.375$  GHz was modulated on a wavelength of  $\lambda = 1577$  nm using a Mach-Zehnder modulator and an arbitrary waveform generator. It was injected to the transistor-outline EML at a power level of -12 dBm, which locks its DFB emission to the downlink wavelength. As reported in [9], stable locking can be achieved even for a much lower power level of -30 dBm, provided that both involved DWDM wavelengths are temperature-stabilized through a micro-Peltier element. The EAM is biased at -0.7V, which operates as semi-transparent photodiode/modulator. The uplink OFDM radio utilizes the same RF carrier frequency  $f_{RF}$  and is launched by the EML with variable RF drive in order to evaluate the corresponding downlink reception penalty. An optical circulator separates the down- and uplink before the uplink is received by an APD for a fixed optical budget (OB) of 15 dB.

The OFDM radio signals for down- and uplink were de-correlated with respect to modulation format and time. We used 16- and 64-QAM modulation for the 128 OFDM sub-carriers of the down- and uplink, respectively. All sub-carriers in both, down- and uplink, were used for data transmission, except for three that are dedicated to pilot information. The OFDM bandwidth was 62.5 MHz according to the presently accomplished peak-isolation bandwidth of the bleed-cancelling circulator. After digitization through a real-time scope, the feed-forward uplink cancellation for the downlink takes the frequency response ripple between DAC and ADC and the pilot tones of the uplink bleed into account by spectrally shaping the forwardly fed uplink and by further adjusting its magnitude.

Typical RF spectra for the received down- and uplink are presented in Fig. 3a. First, the OFDM spectra are clearly delimited due to the coherent homodyne detection through the EML. Second, the uplink ( $v$ ) also shows a crosstalk component from the downlink. This is due to the reflection of the downlink that is specific to the EML receiver. It necessitates a similar feed-forward cancellation at the uplink reception, though it is not seen as very practical due to the nature of the reflected downlink as time-delayed far-end crosstalk. Its mitigation would require a re-design for the coherent EML receiver, together with means for its polarization-independent operation. Concerning the second aspect, the current experiment has employed manual polarization control (PC in Fig. 2b) for the single-polarization EML receiver. However, polarization-independent reception has been demonstrated earlier [10].

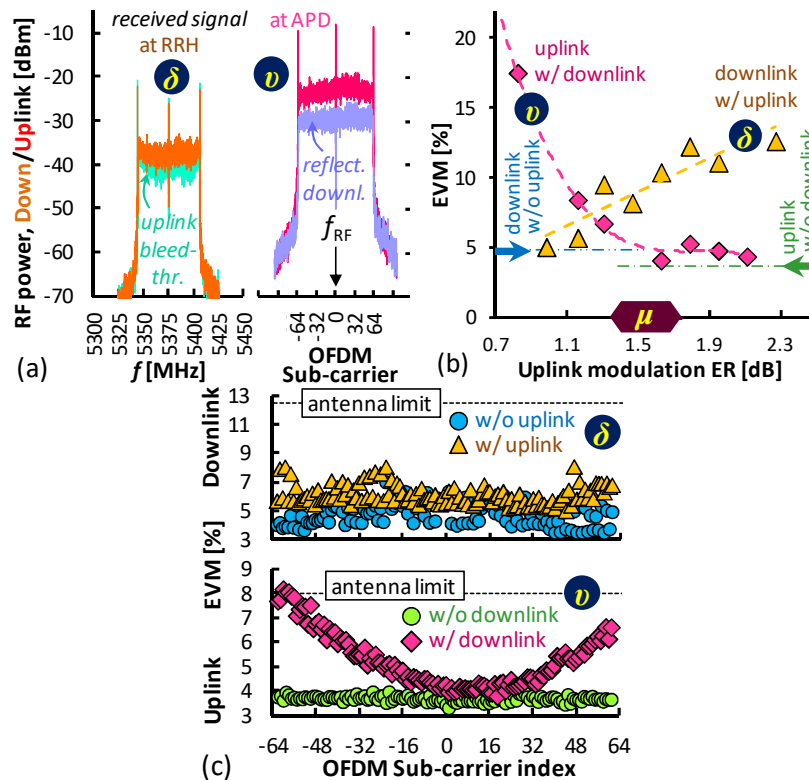


Fig. 3. (a) Received down- ( $\delta$ ) and uplink ( $v$ ) spectra. (b) EVM for down/uplink as function of the uplink modulation ER. (c) EVM per subcarrier.

#### 4. In-Band Crosstalk Noise Suppression for Down- and Uplink: Results and Discussion

Figure 3b reports the full-duplex EVM performance for the down- ( $\delta$ ,  $\blacktriangle$ ) and uplink ( $v$ ,  $\blacklozenge$ ) after the hybrid analogue / digital in-band crosstalk noise suppression for a received optical downlink power of -12 dBm (OB = 15 dB). The half-duplex performance is indicated through arrows. The average downlink EVM without uplink transmission is as low as 4.8%. When activating the uplink, the EVM raises with the uplink launch power, as expressed in Fig. 3b in terms of modulation extinction ratio (ER). The EVM remains within the antenna limit of 12.5% for 16-QAM OFDM transmission, up to an uplink ER of 2.1 dB. Although this ER seems to be rather low at first, it approaches the typical 3-dB value as often adopted in earlier wired access works on wavelength-reuse schemes. More importantly, this ER value is sufficiently high to guarantee reception of the 64-QAM OFDM uplink at a very low EVM of 4.4% ( $\blacklozenge$ ) for an APD input of -10.5 dBm (OB = 15 dB). This is close to the EVM of 3.7% as found for half-duplex uplink

transmission. The uplink EVM degrades when reducing the uplink drive, and surpasses the EVM limit of 8% at a reduced uplink ER of 1.15 dB. For an upstream ER range between 1.3 and 1.8 dB, the joint EVM margin towards the antenna limits is larger than 2% ( $\mu$  in Fig. 3b). For this condition, Fig. 3c presents the EVM per subcarrier for the down- ( $\delta$ ,  $\blacktriangle$ ) and uplink ( $v$ ,  $\blacklozenge$ ), with the corresponding constellations being reported in Fig. 4. Comparison is made between full- ( $\blacktriangle$ ,  $\blacklozenge$ ) and half-duplex transmission ( $\bullet$ ). The EVM increase shown in the uplink EVM of Fig. 3c towards lower and upper OFDM sub-carriers is believed to stem from a sub-optimal far-end downlink crosstalk noise cancellation.

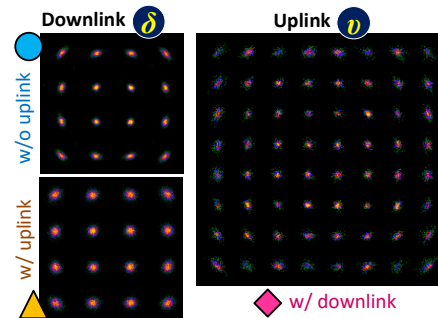


Fig. 4. Constellations for down- ( $\delta$ ) and uplink ( $v$ ).

## 5. Conclusion

We experimentally demonstrated a full-duplex RRH transceiver, using only a single-port modulator/detector device at the optical layer. EVM margins beyond 2% have been achieved for full-duplex 16-QAM/64-QAM OFDM down/uplink radio transmission at the same RF carrier frequency, thanks to the hybrid analogue/digital mitigation of in-band crosstalk noise. Wider operation bandwidths for the bleed-cancelling circulator are expected for a higher scale of RF circuit integration with optimized balancing. Millimeter-wave operation is left for future investigation.

*Acknowledgement:* This work was supported by the ERC under the EU Horizon-2020 programme (grant agreement No 804769).

## 6. References

- [1] I. Alimi et al., "Toward an Efficient C-RAN Optical Fronthaul for the Future Networks," *IEEE Comm. Surv. Tut.* **20**, 708-769 (2018).
- [2] M. Sung et al., "Demonstration of IFoF-Based Mobile Fronthaul in 5G Prototype With 28-GHz Millimeter wave" *JLT* **36**, 601-609 (2018).
- [3] K. Kanta et al., "Analog fiber-wireless downlink transmission of IFoF/mmWave over in-field deployed legacy PON infrastructure for 5G fronthauling," *JOCN* **12**, 57-65 (2020).
- [4] Q. Nguyen et al., "Multi-Functional R-EAM-SOA for 10-Gb/s WDM Access," in *Proc. OFC, Los Angeles, USA, Mar. 2011, OThG7*.
- [5] M. Raj et al., "Design of a 50-Gb/s Hybrid Integrated Si-Photonic Optical Link in 16-nm FinFET," *J. Solid-State Circ.* **55**, 1086 (2020).
- [6] A. Stöhr et al., "Full-Duplex Fiber-Optic RF Subcarrier Transmission Using a Dual-Function Modulator/Photodetector," *IEEE Trans. Microwave Theory Techniques* **47**, 1338-1341 (1999).
- [7] B. Schrenk, "The EML as Analogue Radio-over-Fiber Transceiver – a Coherent Homodyne Approach," *JLT* **37**, 2866-2872 (2019).
- [8] M.P. Thakur et al., "480-Mbps, Bi-Directional, Ultra-Wideband Radio-Over-Fiber Transmission Using a 1308/1564-nm Reflective Electro-Absorption Transducer and Commercially Available VCSELs," *JLT* **27**, 266-272 (2009).
- [9] B. Schrenk et al., "A Coherent Homodyne TO-Can Transceiver as Simple as an EML," *JLT* **37**, 555-561 (2019).
- [10] B. Schrenk et al., "Simple Laser Transmitter Pair as Polarization-Independent Coherent Homodyne Detector," *OpEx* **27**, 13942 (2019).